Available online at www.sciencedirect.com

ScienceDirect

Energy Procedia 152 (2018) 556–561

Energy Procedia

www.elsevier.com/locate/procedia

CUE2018-Applied Energy Symposium and Forum 2018: Low carbon cities and urban energy systems, 5–7 June 2018, Shanghai, China

Research on Modeling and SOC Estimation of Lithium Iron Phosphate Battery at Low Temperature

Jian Wu[a], Tong Li[a], Hao Zhang[b], Yanxiang Lei[a], Guangquan Zhou[a]

[a]National Active Distribution Network Technology Research Center, Beijing Jiaotong University, Beijing, 100044, China
[b]CRRC QINGDAO SIFANG CO.,LTD, Qingdao, 266111, China

Abstract

The battery model is the basis for battery status estimation, and its accuracy will have a direct impact on accuracy of status estimation. In the field of rail transit, the reasonable allocation of battery capacity in conjunction with the actual operating conditions of the train also requires to establish an accurate battery model. Current battery models rarely consider the effect of temperature on model parameters. However, in some areas, it is very likely to encounter extremely cold conditions while the train is in motion. Firstly, taking into account the effects of temperature on available battery capacity, open-circuit voltage, ohm resistance, and polarization parameters, this article constructed a new battery model suitable for low temperature and small rate discharge conditions based on the lithium iron phosphate battery that used in the project. Then, this paper built a battery model in Matlab/Simulink and verified the accuracy of it through simulation. After that, this paper used extended Kalman filter (EKF) algorithm to estimate the state of change (SOC) at different temperatures and carried out simulation verification. Simulation results showed that the battery model and the SOC estimation method established in this paper had higher estimation accuracy in low-temperature environment.

Selection and peer-review under responsibility of the scientific committee of the CUE2018-Applied Energy Symposium and Forum 2018: Low carbon cities and urban energy systems.

Keywords: Low temperature; Lithium iron phosphate battery; SOC estimation; Extended Kalman filter algorithm

1. Introduction

In recent years, lithium iron phosphate batteries have been widely used in new energy vehicles and power grids due to their small size, long service life, high current discharge, and maintenance free [1]. However, when battery works in a low-temperature environment, its internal characteristics and capacity will be changed, at this time, if battery capacity and parameters cannot be adjusted in real time based on current temperature, accuracy of the battery model will be greatly affected, which will affect the SOC estimation accuracy. Therefore, it is important to study the

Selection and peer-review under responsibility of the scientific committee of the CUE2018-Applied Energy Symposium and Forum 2018: Low carbon cities and urban energy systems.
10.1016/j.egypro.2018.09.210

battery modeling and the SOC estimation method at low temperature, which is of great significance for battery to operate safely and maximize the battery power performance under different temperature conditions.

Reference [1] provided several common model methods for lithium iron phosphate batteries and validated the accuracy of the model. Low et al. presented an improved model comprising two resistance–capacitance (RC) parallel networks in [2], which gave a good prediction with sufficient accuracy for lithium iron phosphate batteries. To enhance the model adaptability to high rates and model suitability to system simulation, a hybrid battery model was presented in [3], which utilized a kinetic model to represent the rate capacity effect instead of the highly coupled diffusion model，but did not considerate with temperatures. Reference [4] used the improved Nernst equation standard battery chemistry process in which the parameters in the equation are related to temperature. A completed cell-level electrical equivalent circuit model (ECM) of energy and power lithium-ion cells with 3 different chemistries and multiple temperatures was developed in reference [5], specifically when the extended coulomb counting technique is implemented. Reference [6] introduced the temperature compensation coefficient to correct actual usable capacity of the battery at low temperature, but did not analyse the change of available capacity from the internal mechanism of the battery. A battery model at low temperature based on the Nernst electrochemical equation was established in [7], but the paper did not analyse effects of temperature on the polarization process. Based on the analysis for the mapping relationship between battery parameters and its SOC, a three dimensional response surface open circuit voltage model was proposed in reference [8] for correcting erroneous SOC estimation and giving accurate estimations of cell state-of-charge for series-connected battery pack. Reference [9] provided several SOC estimation methods. Among them, the extended Kalman filter algorithm evaded the problem that the initial SOC could not be calibrated and the current accumulated error was difficult to eliminate in the Ampere-hour integration method. Reference [10] proposed to correct initial SOC value by using the open circuit voltage after fully standing, but the flat OCV-SOC curves of the lithium iron phosphate battery did not have much significance for the correction of ampere-hour integral method [11].

In view of above problems, this paper established a lithium iron phosphate battery model had based on low-temperature by calibrating battery capacity and identifying battery parameters. Then, this paper built a battery model in Matlab/Simulink and verified the accuracy of the battery model through simulation. On this basis, this paper used extended Kalman filter algorithm to estimate the state of change (SOC) at different temperatures and carried out simulation verification.

2. Proposed Model and Experimental Setup

The first-order equivalent circuit model, also known as the Thevenin equivalent circuit model, is the most common battery model. However, it only uses the first-order RC loop to reflect the polarization process of the battery. The second-order RC model adds a first-order RC loop bases on the Thevenin model, which can describe the electrochemical polarization and concentration polarization processes, respectively. Therefore, in order to more effectively describe effects of different temperatures on battery performance, This paper selected the second-order RC model to build a lithium iron phosphate battery model at low temperature, the model is shown in Fig.1.

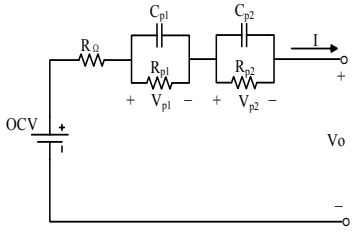

Fig.1. The second-order RC model

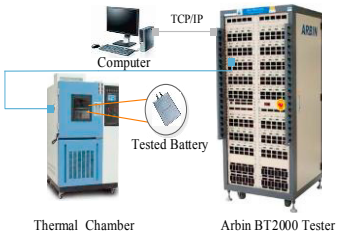

Fig.2. Experimental equipment

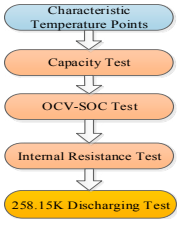

Fig.3. Experiment flowchart

This paper used ATL-78Ah lithium iron phosphate battery cell as the experimental object. At the same time chose the high-low temperature test box, charge-discharge test equipment to build battery experimental platform. The unit of temperature in this paper used the international unit Kelvin. In the range of 253.15K to 298.15K, five

characteristic temperature points of 253.15K, 263.15K, 273.15K, 283.15K, and 298.15K were used to calibrate battery capacity and identify parameters.

The project had required that the discharge temperature of the battery was not less than 253.15K and the ratio was not more than 0.5C when the ambient temperature was below zero, so accorded to requirements of the project and the temperature rise, the discharge current of the paper was 0.2C. In addition, the lithium iron phosphate battery is forbidden to be charged at any rate when it is less than zero. This paper only considered the effect of low temperature on the discharge performance of lithium iron phosphate battery. All charging experiments were under 298.15K, and the current followed the charge standard of the cell specification. The flowchart of the experiment is shown in Figure.3, and specific experimental steps for capacity testing and parameter identification at different temperatures were the same as test methods in [12].

3. Model Extraction

3.1. Battery Capacity Model at Low Temperature

Capacity is an inherent property of lithium batteries. The temperature-induced capacity reduction can continue to be supplemented with a small rate current discharge after fully standing. However, there is no long-term standing condition in actual conditions, and too small current cannot meet the power requirements of the train. Based on above facts, when discharging under the same condition as 298.15K, the maximum capacity that the battery can discharge uninterruptedly was defined as the maximum available capacity of the battery at the current temperature. The actual usable capacity of the battery at five characteristic temperature points is shown in Table 1.

Table 1. The actual usable capacity of the battery.

Temperature(K)	253.15	263.15	273.15	283.15	298.15
Capacity(Ah)	49.2	65.5	75.5	76.3	78

This paper used Arrhenius equation [13] to fit the battery's actual usable capacity curve at different temperatures.

$$Q_t = Q_0 \times a \times \exp\left(-b/t\right) + c \tag{1}$$

In(1), Q_0 (Ah) is the battery discharge capacity at 298.15K; T is the actual ambient temperature; a, b, c are parameters that need to be identified; Parameter ‘b’ reflects the activation energy of reactants. In the collision theory, it is considered that ‘b’ is a constant that is not related to temperature, but it can be seen from the expression that ‘b’ is at the exponential position, and the lower the temperature, the more severe influence is the activation energy of the material causes. This paper supplemented the capacity test experiment at 268.15K. The capacity curve below 273.15K was fitted to the measured capacity at four temperature points of 253.15K, 263.15K, 268.15K, and 273.15K; the capacity curve above 273.15K was based on the test capacity at 273.15K, 283.15K, and 298.15K.

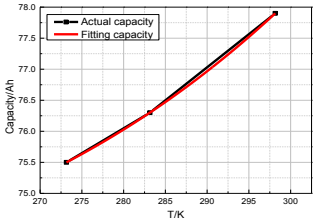

Fig. 4 The capacity fitting curve at below 273.15K

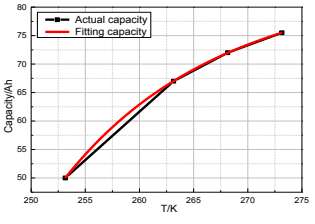

Fig. 5 The capacity fitting curve at above 273.15K

The capacity fitting curve at below and above 273.15K separately show that using Arrhenius formula to estimate the available capacity at low temperature can obtain more accurate results. The capacity fitting value is 57.5Ah at 258.15K. Compared with the experimental test capacity of 58.05Ah, the relative error is 0.9%.

3.2. OCV-SOC Curves and Parameters Identification

Battery characteristic parameters can be viewed as a function of SOC, which means that parameters in the battery model are often linearly interpolated according to parameters identification by some given SOC feature points. However, the effect of temperature on the cell performance is non-linear, battery parameters at different temperatures obtain by linear interpolation will have large errors.

The Nernst equation [3] indicates that there is a quantitative relationship between the electromotive force and the ions that are participating in the reaction:

$$U_{oc}[SOC(t)] = a(t) + b(t) \times \ln\left(SOC(t)\right) + c(t) \times \ln\left(1 - SOC(t)\right) \tag{2}$$

In (2), $a(T)$ $b(T)$ and $c(T)$represent coefficients of the OCV-SOC equation at different temperatures. Had Based on identification results of five characteristic temperatures with eleven SOC characteristic points, this paper used the least squares method to obtain coefficients $a(T)$, $b(T)$ and $c(T)$. Parameters did not change significantly between two temperatures, so parameters a, b, and c at the unknown temperature point in the model were obtained by piecewise linear interpolation from a, b, and c at the characteristic temperature points

Fig. 6 shows OCV-SOC fitting curves for various feature temperature points.

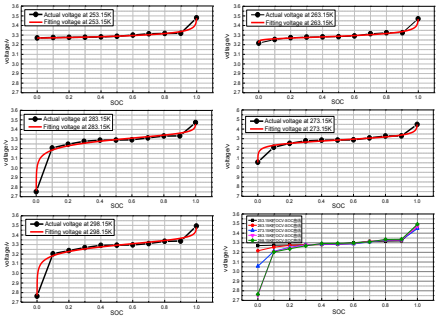

Fig.6. OCV-SOC fitting curves

Since above formula did not describe the open circuit voltage when the battery was fully charged or empty, it had large deviations at the high and low ends of the SOC. This article used above formula only in 10%-70% SOC for open circuit voltage fitting, the open circuit voltage of other SOC intervals were still obtained by piecewise linear interpolation according to SOC feature points.

$$\begin{cases} U_{oc}[SOC(t)] = a(t) + b(t) \times \ln\left(SOC(t)\right) + c(t) \times \ln\left(1 - SOC(t)\right), & 10\% < SOC < 70\% \\ U_{oc}[SOC(t)] = a \times SOC(t) + b, & SOC < 10\% \text{ or } SOC > 70\% \end{cases} \tag{3}$$

The ohm resistance of each SOC feature point in this paper was obtained by the voltage jump within 1 second of the starting current; and the polarization resistance and the polarization capacitance are obtained by the least-square method identification[12] based on the polarization voltage expression in the 2.2.

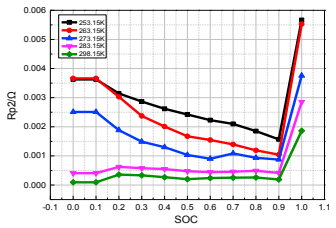

Fig.7(1). The ohmic resistance

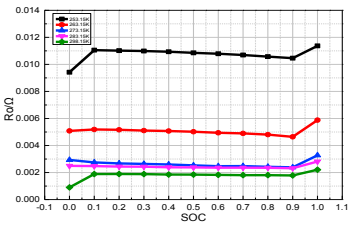

Fig.7(2) The polarization resistance

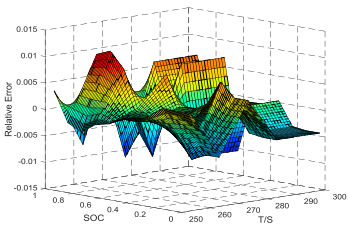

Fig. 8. Fitting error of resistance

Fig.7 and Fig. 8 are results of resistances. According to the results of resistance identification, ohm resistance and electrochemical polarization resistance are significantly affected by temperature, especially in the 0-10% and 90%-100% SOC interval. Therefore, the battery should be avoided to work in the high and low end SOC ranges. Electrochemical transfer impedance and ohm resistance were obtained by least squares fitting based on Arrhenius equation, the concentration polarization resistance was too less affected by temperature to obtain by linear interpolation.

Based on the Matlab/Simulink simulation platform, this paper set up the battery second-order RC model. The experimental data was obtained by the sampling period of 1 second when battery was discharged according to method in chapter 2 at 258.15K. The simulation model also used the temperature condition of 258.15K. When performing simulation verification, the paper took the current-time curve as input quantity, then took the terminal voltage as the output result.

Simulation results are shown in Figure.9 and Figure.10. Results show that when SOC is in the range of 90%-100%, due to abrupt changes in the open circuit voltage and polarization parameters, model error is large. Considered that SOC is seldom at both ends in engineering practice, this paper ignored error that in 90%-100% SOC. Compared with the measured voltage, the following error of the terminal voltage in the second-order RC model is less than 1% in 6000s in Fig. 10. It can be seen that the above model has high precision.

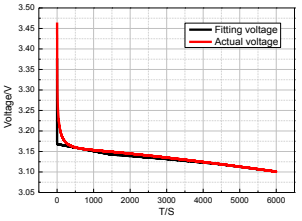

Fig. 9. Fitting voltage and actual voltage

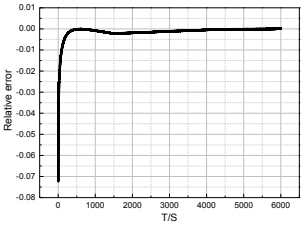

Fig. 10. Relative error of the terminal voltage

4. SOC Estimation at Low Temperature

Battery state of charge (SOC) is an important parameter for evaluating the mileage of new energy electric vehicles and new energy trams. The SOC in this paper was uniformly defined as the ratio of the current available capacity at the current temperature to the maximum available capacity at the same temperature. Based on the battery model and parameter identification methods which had established in chapter 3, the extended Kalman filter algorithm [14] was used to estimate the SOC of the battery at different temperatures. Since battery parameters change greatly at both ends of the SOC, the SOC estimation is still using the Ampere-hour integration method when the SOC is in 0%-20%.

The key steps of the extended Kalman filter algorithm had been elaborated in [14] and it would not be repeated here. In particular, System parameter which used to solve the Kalman gain ignored the influence of the SOC range on the ohmic internal resistance and polarization parameters, and only considered the derivative of OCV to SOC.

According to the open circuit voltage of different SOC points, the system parameter of the i-th SOC feature point is:

$$H_i = \frac{OCV(i) - OCV(i-1)}{SOC(i) - SOC(i-1)} \tag{4}$$

This paper only calculated ‘H’ with known temperature and SOC points, for unknown temperature and SOC points, ‘H’ were still interpolated from known points.

Based on writing .M programs in MATLAB to verify the Kalman filter algorithm, this paper obtained the experimental data by the sampling period of 1 second when the battery was discharged according to 2.1 at 258.15K. Arbin embeds the current integration method. So we got the benchmark SOC based on the discharge capacity obtained by Arbin.

SOC estimation curves are shown in Fig.11. Operation results show that the SOC estimation error is less than 2%. And errors mainly came from errors of the model and the system parameter ‘H’.

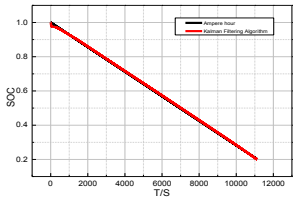

Fig.11. SOC estimation curve

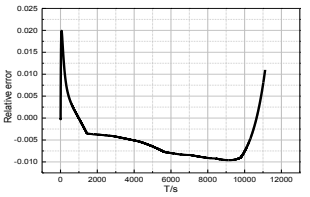

Fig.12. SOC error curve

5. Conclusion

This paper established a battery model of the lithium iron phosphate battery suitable for different temperatures, and then simulated the model combined with specific working conditions. The simulation results show that the model has a good tracking capability for the battery terminal voltage, and the average relative error is less than 1%. At the same time, this paper presented a method for estimating SOC using Kalman filtering algorithm at low temperature. The SOC estimation error is within 2%. Lack of consideration of coupling effects on discharge rate and temperature for battery performances is the inadequacy of this paper. The coupling effects of them will be conducted in subsequent studies.

Acknowledgements

This work was supported by the National Key Technology Research and Development Program of the Ministry of Science and Technology of China under Grant No.2015BAG 12B01.

References

[1] Yang Y, Zheng F. Study on Model of LiFePO4 Batteries Used by Electric Vehicles[D]. Xidian University, 2015.
[2] Liu X, Sun Z, He Y, et al. SOC estimation method based on lithium-ion cell model considering environmental factors[J]. Journal of Southeast University, 2017.
[3] Low W Y, Aziz J A, Idris N R N, et al. Electrical model to predict current–voltage behaviours of lithium ferro phosphate batteries using a transient response correction method[J]. Journal of Power Sources, 2013, 221(1):201-209.
[4]Yang D, Wang Y, Pan R, et al. State-of-health estimation for the lithium-ion battery based on support vector regression[J]. Applied Energy, 2017.
[5] Kim T, Qiao W. A Hybrid Battery Model Capable of Capturing Dynamic Circuit Characteristics and Nonlinear Capacity Effects[J]. IEEE Transactions on Energy Conversion, 2011, 26(4):1172-1180.
[6] Nikolian A, Jaguemont J, Hoog J D, et al. Complete cell-level lithium-ion electrical ECM model for different chemistries (NMC, LFP, LTO) and temperatures (−5 °C to 45 °C) – Optimized modelling techniques[J]. International Journal of Electrical Power & Energy Systems, 2018, 98:133-146.
[7] Yao H E, Cao C R, Liu X T, et al. SOC estimation method for lithium battery based on variable temperature model[J]. Electric Machines Control, 2018.
[8] Miao Z, Study on Dynamic Characteristics and SOC Estimation of Power Lithium Ion Batteries [D]. Harbin Institute of Technology, 2017.
[9] Sun F, Xiong R. A novel dual-scale cell state-of-charge estimation approach for series-connected battery pack used in electric vehicles[J]. Journal of Power Sources, 2015, 274:582-594.
[10] Chen X, Yu H, An improved amp-open circuit voltage estimation SOC[J]. BeijingAutomotiveEngineering, 2016(4):33-37.
[11] Ma Z, Jiang J, Wang Z, et al. A Research on SOC Estimation for LiFePO_4 Battery with Graphite Negative Electrode Based on Incremental Capacity Analysis[J]. Automotive Engineering, 2014.
[12] Liu S, Jiang J, Shi W, et al. Butler–Volmer-Equation-Based Electrical Model for High-Power Lithium Titanate Batteries Used in Electric Vehicles[J]. IEEE Transactions on Industrial Electronics, 2015, 62(12):7557-7568.
[13] Lai S, Liu S, Xu Y, Discussion about Arrhenius Formula[J]. Guangdong Chemical Industry, 2016(17):80-81.
[14] Li Z, Zhao Y, EV battery management system and accurate estimation of SOC[J]. Chinese Journal of Power Sources, 2016, 40(5):1090-1093.